

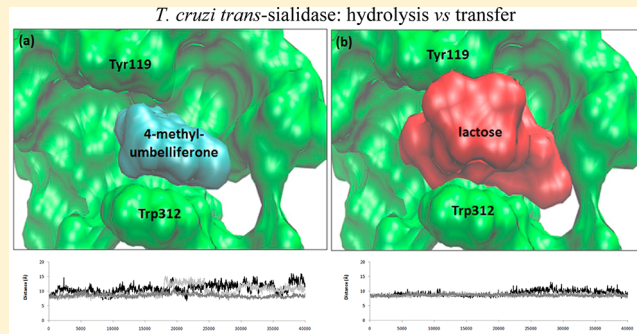
# Insights into the Activity and Specificity of *Trypanosoma cruzi* trans-Sialidase from Molecular Dynamics Simulations

Felicity L. Mitchell,<sup>†</sup> João Neres,<sup>†,§</sup> Anitha Ramraj,<sup>‡</sup> Rajesh K. Raju,<sup>‡</sup> Ian H. Hillier,<sup>‡</sup> Mark A. Vincent,<sup>‡</sup> and Richard A. Bryce\*,<sup>†</sup>

<sup>†</sup>School of Pharmacy and Pharmaceutical Sciences and <sup>‡</sup>School of Chemistry, University of Manchester, Oxford Road, Manchester M13 9PT, U.K.

Supporting Information

**ABSTRACT:** *Trypanosoma cruzi* trans-sialidase (TcTS), which catalyzes the transfer or hydrolysis of terminal sialic acid residues, is crucial to the development and proliferation of the *T. cruzi* parasite and thus has emerged as a potential drug target for the treatment of Chagas disease. We here probe the origin of the observed preference for the transfer reaction over hydrolysis where the substrate for TcTS is the natural sialyl donor (represented in this work by sialyllactose). Thus, acceptor lactose preferentially attacks the sialyl-enzyme intermediate rather than water. We compare this with the weaker preference for such transfer shown by a synthetic donor substrate, 4-methylumbelliferyl  $\alpha$ -D-acetylneuraminate. For this reason, we conducted molecular dynamics simulations of TcTS following its sialylation by the substrate to examine the behavior of the asialyl leaving group by the protein. These simulations indicate that, where lactose is released, this leaving group samples well-defined interactions in the acceptor site, some of which are mediated by localized water molecules; also, the extent of the opening of the acceptor site to solvent is reduced as compared with those of unliganded forms of TcTS. However, where there is release of 4-methylumbelliferonone, this leaving group explores a range of transient poses; surrounding active site water is also more disordered. The acceptor site explores more open conformations, similar to the case in which the 4-methylumbelliferonone is absent. Thus, the predicted solvent accessibility of sialylated TcTS is increased when 4-methylumbelliferyl  $\alpha$ -D-acetylneuraminate is the substrate compared to sialyllactose; this in turn is likely to contribute to a greater propensity for hydrolysis of the covalent intermediate. These computational simulations, which suggest that protein flexibility has a role in the transferase/sialidase activity of TcTS, have the potential to aid in the design of anti-Chagas inhibitors effective against this neglected tropical disease.



Enzymes are efficient biological catalysts of remarkable specificity. Details of the exact means by which enzymes function, however, are still not thoroughly understood. Historically, proposals have included the lock-and-key,<sup>1</sup> induced fit,<sup>2</sup> and conformational selection models.<sup>3</sup>

The *Trypanosoma cruzi* trans-sialidase (TcTS) enzyme is a member of the sialidase family (EC 3.2.1.18), members of which catalyze the hydrolysis of terminal sialic acid residues.<sup>4</sup> TcTS is crucial to the development and proliferation of the *T. cruzi* parasite.<sup>5–7</sup> It has thus emerged as a potential drug target for the treatment of Chagas disease, which is estimated to affect 10–12 million Latin Americans.<sup>8</sup> Of the infected patients who go on to develop clinical manifestations, more than 15000 die each year, most commonly because of cardiac complications.

Because *T. cruzi* is unable to synthesize its own sialic acids,<sup>9</sup> it instead employs TcTS to scavenge these residues from the glycoconjugate host onto its own surface mucins.<sup>10</sup> Thus surface sialylation is essential for evasion from the host immune system.<sup>11</sup> Unlike most sialidases, TcTS is uniquely efficient at preferentially transferring sialic acids from the terminus of

donor glycoconjugates rather than hydrolyzing them.<sup>5,12–16</sup> For example, with a sialyllactose donor substrate, the transfer of a sialyl group to the lactose acceptor to yield the sialyllactose as the product is ~5 times more efficient than hydrolysis to liberate sialic acid (Table 1).<sup>4</sup>

A growing body of evidence suggests that, for some enzymes, there is an interplay between catalysis and protein conformational flexibility, with the involvement of dynamical processes and atomic motions in the precise alignment of the substrate with the enzyme (as reviewed by Benkovic<sup>17</sup>). The sialidase family of enzymes is no exception to this notion, with a growing body of studies implying active site flexibility in their mode of action.<sup>18–22</sup>

The currently accepted mechanism of action of TcTS is depicted in Scheme 1, in which sialyllactose is shown as the representative donor substrate. The enzyme follows a ping-

Received: August 16, 2012

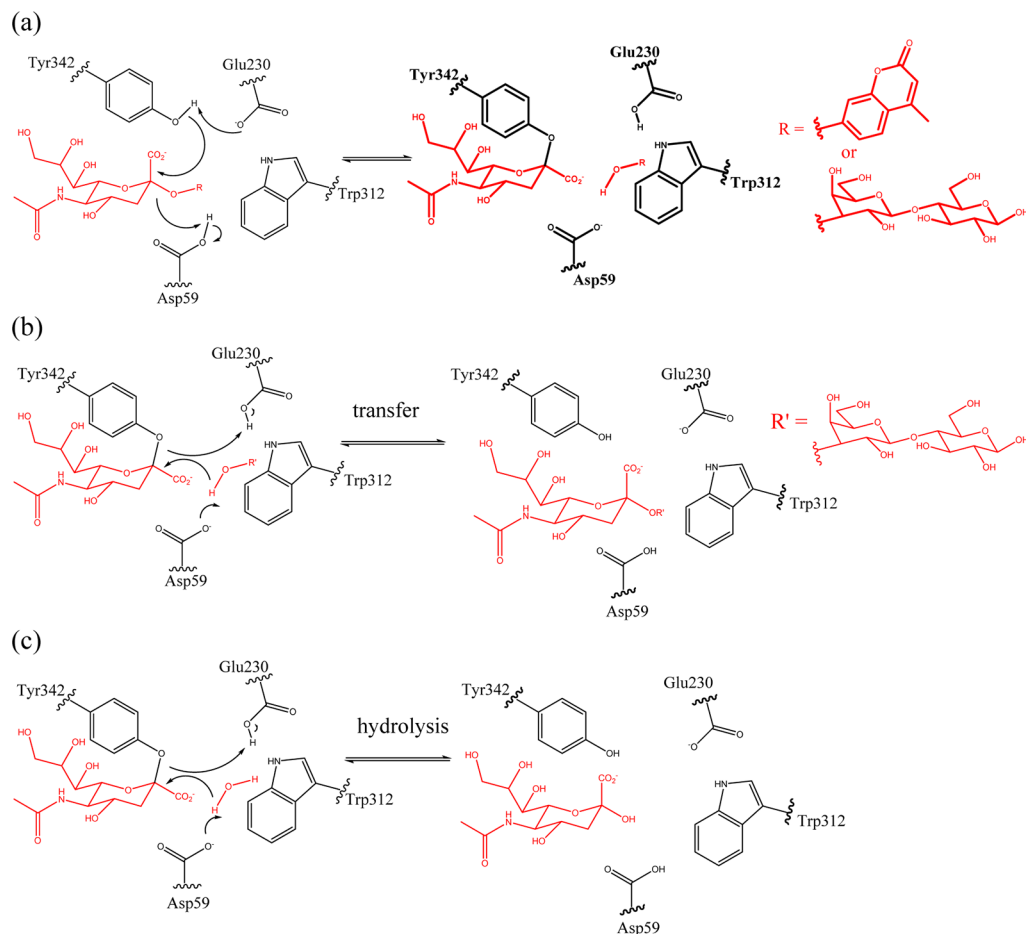
Revised: April 13, 2013

Published: May 14, 2013

**Table 1.** Donor Substrates, Aglycon Leaving Groups, and Rates of Hydrolysis and Transfer to Lactose (in nanomoles of sialic acid per minute per milligram) Catalyzed by TcTS<sup>4</sup>

donor substrate	leaving group	rate of hydrolysis	rate of transfer to acceptor	ref
		306.0±4.4	1412.98±21.95	4
		599.1±16.5	860.89±18.30	4

**Scheme 1.** Putative Mechanism of TcTS<sup>a</sup>



<sup>a</sup>(a) Using either sialyllactose or 4-methylumbelliferyl  $\alpha$ -D-acetylneuraminate (MuNANA) as a donor substrate (red), formation of the TcTS–sialyl covalent intermediate occurs, also producing lactose or Mu (ROH), respectively. The two TcTS–sialyl/ligand systems on the right-hand side of panel a are the principle focus of our MD studies here (marked in bold) and provide the branch point for subsequent (b) transfer of a sialyl group from TcTS to lactose as the acceptor R'OH (note that the left-hand side of panel b is identical to the right-hand side of panel a when ROH = lactose), or (c) hydrolysis to release sialic acid, preferred to a greater extent when the substrate is MuNANA than when it is sialyllactose (i.e., when the righthand side of panel a has ROH = Mu).

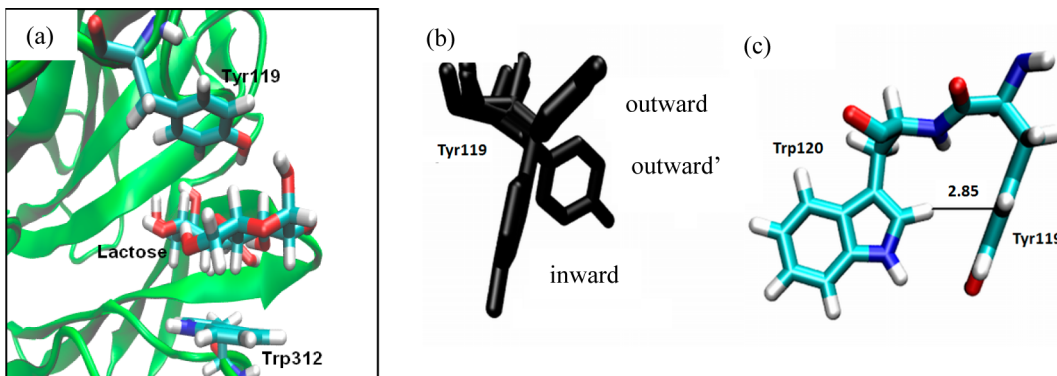


**Figure 1.** (a) Lactose bound in the acceptor site of TcTS. (b) Conformations of Tyr119 from MD simulations. (c) Interaction of Tyr119 with Trp120. MD average distance is given in Ångstroms.

pong bi-bi kinetic mechanism with formation of a sialyl-enzyme intermediate (Scheme 1a).<sup>23</sup> Evidence suggests that Asp59 functions as the acid–base catalyst in this glycosidase and that the active site nucleophile, Tyr342, covalently binds the donated sialic acid to form the sialyl-enzyme intermediate.<sup>21,23,24</sup> The resulting asialyl glycoconjugate, which is lactose for the sialyllactose donor substrate, is liberated from the active site [leaving group (Table 1)], while the covalent intermediate persists until a suitable acceptor molecule is found. The sialic acid moiety is then transferred onto the bound acceptor molecule by the reverse mechanism, shown in Scheme 1b as another molecule of lactose. Alternatively, when the covalent intermediate is preferentially attacked by water, hydrolysis occurs with release of sialic acid (Scheme 1c).

The overall catalytic reaction of TcTS proceeds with retention of the anomeric configuration at C2 of the sialyl residue. Only  $\alpha$ -(2,3)-linked sialic acids are transferred to terminal  $\beta$ -galactosyl acceptors,<sup>5,25,26</sup> or alternatively, only  $\alpha$ -sialic acid (and  $\beta$ -sialic acid by subsequent mutarotation) is generated in the event of a hydrolysis reaction, in which water is the acceptor (Scheme 1c).<sup>26,27</sup> Interestingly, TcTS is also capable of transferring sialic acid from non-natural donors such as *p*-nitrophenyl and 4-methylumbelliferyl  $\alpha$ -sialosides, and the fluorogenic substrate 4-methylumbelliferyl  $\alpha$ -D-acetylneuramidine (MuNANA) is widely used in sialidase assays.<sup>4,16</sup> However, the rate of transfer is slower for these artificial substrates than for the natural ligands. Enzymatic studies suggest that the rate of transfer of the sialyl group from MuNANA to lactose is only ~0.6 compared to that for a sialyllactose donor (Table 1),<sup>4</sup> while the rate of hydrolysis of MuNANA by TcTS is ~2 higher than that of sialyllactose (Table 1).<sup>4,16</sup>

The molecular basis of these differences in the reaction of MuNANA and sialyllactose as substrates for TcTS is currently unclear, and an understanding of them is important not only in mechanistic terms but also for the design of TcTS inhibitors<sup>28–30</sup> and engineering of TcTS mutants with altered specificity.<sup>4,31</sup> One proposal for the enhanced hydrolysis of MuNANA suggests occlusion of the acceptor site by the Mu leaving group, preventing the correct orientation of an acceptor molecule as required for successful transfer.<sup>16</sup> Another possibility may be the increased level of solvent exposure of the covalent intermediate during the reaction of TcTS with MuNANA as compared to sialyllactose. Indeed, crystallography<sup>21</sup> and previous molecular dynamics simulations (MD) by us<sup>32</sup> and others<sup>33</sup> indicate that the acceptor site of TcTS can be

flexible. The acceptor site principally consists of Tyr119 and Trp312, which form  $\pi$ -CH and  $\pi$ -OH interactions with incoming acceptor  $\beta$ -galactoside glycoconjugates (Figure 1a). Potential differences in acceptor site flexibility for the enzyme as it reacts with MuNANA as compared to sialyllactose might dictate enhanced solvent accessibility and therefore also influence the preference for hydrolysis relative to transfer.

The observed variations of the rates of hydrolysis and transfer with different substrates (Table 1) imply changes in the activation energies of the rate-determining steps of less than ~3 kcal/mol. The prediction of such small energy differences for the large and complex systems investigated here would require the determination of the full potential energy surface for the different reactions, including conformational averaging, to identify the molecular details of the rate-determining steps, probably by an appropriate quantum mechanics/molecular mechanics procedure.<sup>34,35</sup> As a modest initial start to this extensive computational challenge, we here use MD simulations to probe the relative flexibility of TcTS at a key point in its reaction mechanism, namely immediately after sialylation by MuNANA or sialyllactose, to produce the ROH leaving group (on the right-hand side of Scheme 1a). To this end, we perform triplicate 40 ns MD simulations of the sialylated TcTS covalent intermediate with Mu or lactose present in its acceptor binding site (Figure 1a). It is at this point that the reaction path can follow either hydrolysis to sialic acid or transfer to an acceptor substrate (Scheme 1b,c). For these two systems, we characterize the protein interactions of the leaving group, the degree of ordering in the active site solvent, and the extent of opening of the TcTS acceptor site and quantify the various contributions to the computed binding free energy for interaction of lactose or Mu with sialyl-TcTS. For comparison, we also perform MD simulations of apo TcTS and sialylated TcTS with their acceptor sites unoccupied.

## METHODS

The biomolecular simulation package AMBER 9<sup>36</sup> was used to perform MD simulations of apo TcTS and sialylated TcTS, with and without the acceptor site occupied by either Mu or lactose.

**Model Building.** Multiple crystallographic structures of TcTS are available from the Protein Data Bank (PDB); some of them were modified using MOE<sup>37</sup> and SYBYL<sup>38</sup> to generate the systems studied in this work. These proteins<sup>21,39</sup> were based on a common construct that involved seven surface mutations to improve crystallization but had no effect on transferase and

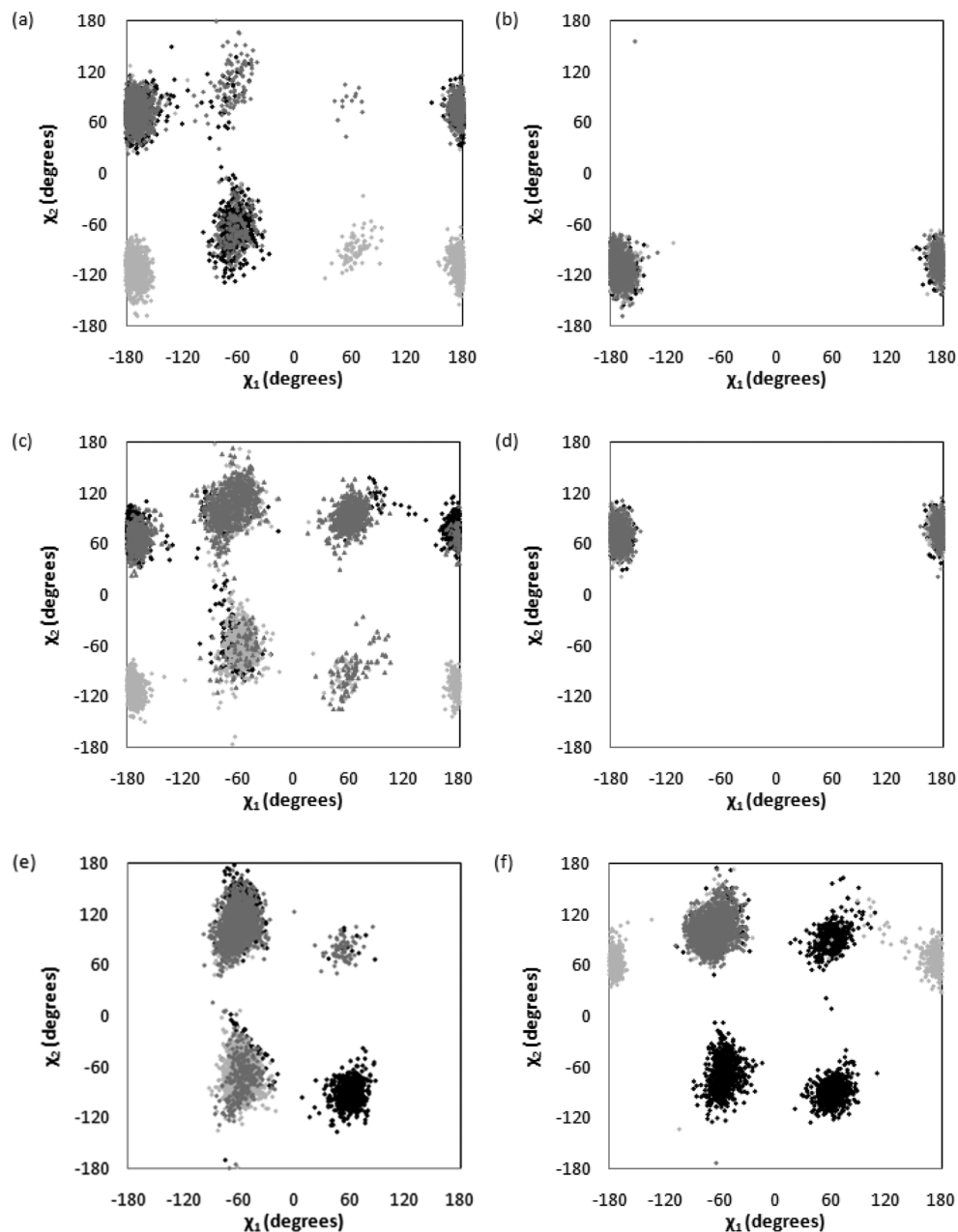


**Figure 2.** Conformations of the Tyr119 side chain during three replicate MD simulations (black, light gray, and dark gray): (a) apo TcTS outward, (b) apo TcTS inward, (c) sialyl-TcTS outward, (d) sialyl-TcTS inward, (e) sialyl-TcTS–lactose conjugate, and (f) sialyl-TcTS–Mu conjugate.

hydrolase activities relative to those of the wild type. The PDB crystallographic structure of the covalent TcTS intermediate (PDB entry 2AH2)<sup>21</sup> was used in the preparation of the sialylated and complexed enzyme systems. Both catalytic and lectin TcTS domains were included in the simulations, and crystallographic water molecules were retained. The fluorine atom at position C3 of the difluorosialic acid, which was required experimentally to trap the covalent intermediate, was replaced *in silico* with a hydrogen atom, and an unresolved flexible loop (residues 399–408) was modeled in and energy minimized. Crystal structures of TcTS indicate active site flexibility,<sup>21,39</sup> in particular that Tyr119 of the acceptor binding site adopts two different orientations: an orientation of Tyr119 that allows it to stack with the acceptor ligand, described by a  $\chi_1$  value of approximately  $-60^\circ$  (Figure 1b), and a downward-pointing orientation of Tyr119, essentially blocking the sialic

acid binding site, with a  $\chi_1$  value of  $180^\circ$ . These conformations, labeled outward and inward, respectively (Figure 1b),<sup>35</sup> are modeled as alternate starting structures for the TcTS systems of this work (Table S1 of the Supporting Information). The conformation of Tyr119 was then manipulated into the inward position when necessary, and the relevant ligand (either lactose from the crystal structure of PDB entry 1MS0<sup>39</sup> or 4-methylumbellifliferone from the crystal structure of PDB entry 1S0J)<sup>21</sup> was transposed into the TcTS acceptor site *in silico* as appropriate. Hydrogen atoms were added and optimized using WhatIf.<sup>40</sup> However, at the covalent intermediate stage in the reaction mechanism, the involvement of Asp59 and Glu230 in the acid–base catalysis of the enzyme results in deprotonation of the former and protonation of the latter (Scheme 1); therefore, these particular residues were modified accordingly (Table S1 of the Supporting Information). The protonation

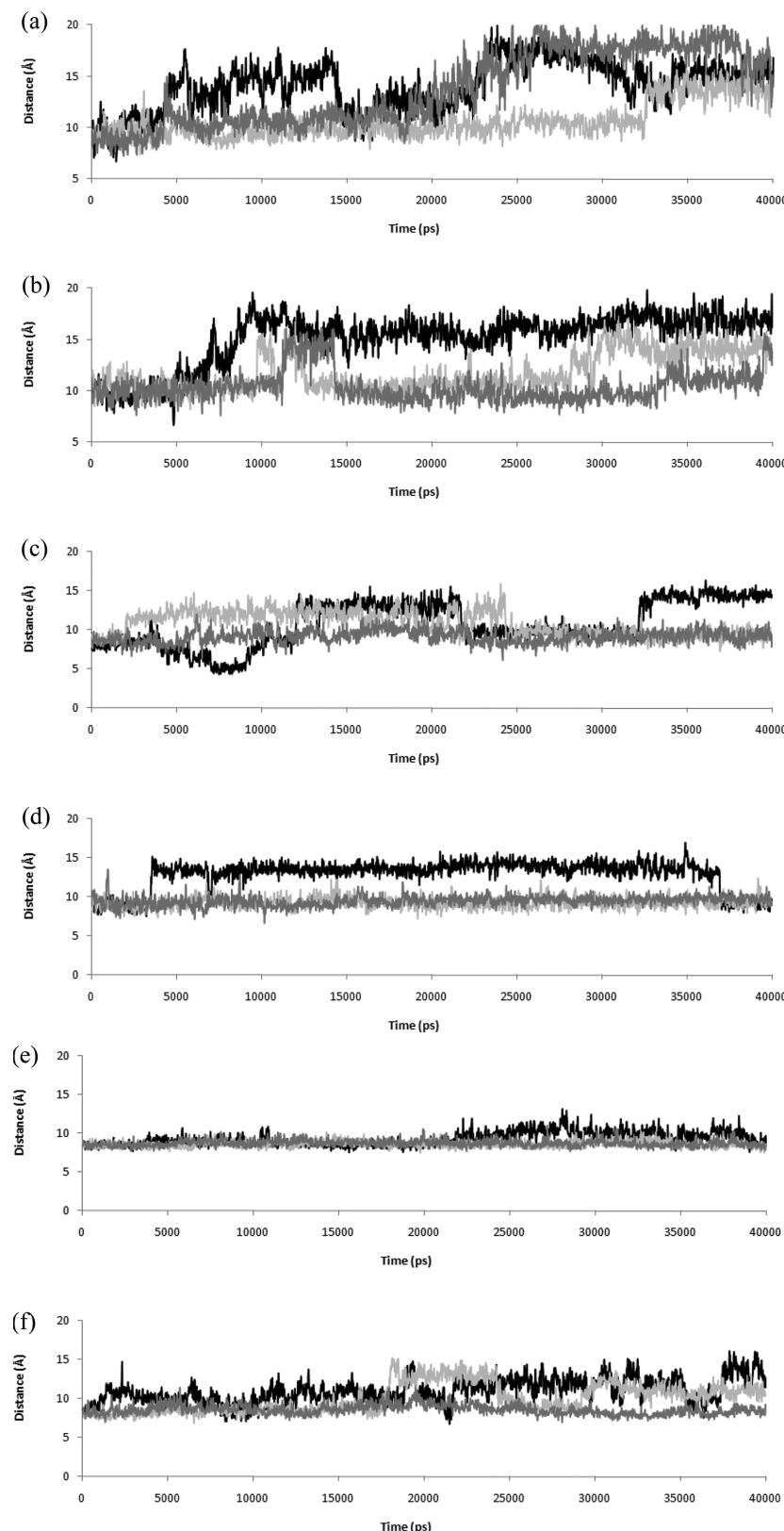


**Figure 3.** Time series of intercentroid distances in Ångstroms between the rings of Tyr119 and Trp312 during three replicate MD simulations (black, light gray, and dark gray): (a) apo TcTS outward, (b) apo TcTS inward, (c) sialyl-TcTS outward, (d) sialyl-TcTS inward, (e) sialyl-TcTS–lactose conjugate, and (f) sialyl-TcTS–Mu conjugate.

state of each of the histidine residues present in the TcTS protein was determined according to the surrounding environment, and a disulfide bond was added between cysteine

residues 396 and 410. The *leap* module of AMBER was used to solvate the system with a truncated octahedron of >24000 TIP3P explicit water molecules.<sup>41</sup>

The AMBER ff03<sup>42</sup> and Glycam06<sup>43</sup> parameter sets were used for protein and sugar, respectively. For the nonstandard 4-methylumbelliflone residue, the *antechamber* module of AMBER was used to perform restrained electrostatic potential (RESP) charge fitting<sup>44</sup> to the HF/6-31G\* electrostatic potential and to obtain the appropriate parameters via the general AMBER force field (*gaff*).<sup>45</sup> Initial structures for the apoenzyme systems were prepared from the crystal structure of PDB entry 1MS3<sup>39</sup> (with Tyr119 in the outward position) or 1MS4<sup>39</sup> (with Tyr119 in an inward pose) in a similar manner. However, in the apoprotein, the protonation states of Asp59 and Glu230 differ from these, the former being neutral and the latter being anionic, as shown in the reaction mechanism (Scheme 1).

**Molecular Dynamics Simulations.** The *sander* module of AMBER was then used to relax the system prior to running production dynamics. Following two stages of heating with weak restraints on the solute(s) of 10 kcal mol<sup>-1</sup> Å<sup>-1</sup>, the system was equilibrated in the isothermal–isobaric ensemble for a further 280 ps, gradually removing restraints. All dynamics employed periodic boundary conditions. The particle mesh Ewald method was used for handling long-range electrostatic interactions,<sup>46</sup> and a cutoff of 8 Å was employed for calculation of nonbonded interactions. The Langevin thermostat was used for temperature control<sup>47</sup> and the Berendsen barostat for pressure control.<sup>48</sup> SHAKE<sup>49</sup> was used to constrain covalent hydrogen bond lengths and allowed a time step of 2 fs. Production dynamics for each system were run for 40 ns. Two additional replicate simulations with a duration of 40 ns were also performed for each of the systems studied, with differing initial velocities. The trajectories acquired are summarized in Table S1 of the Supporting Information and amount to ~0.6 μs of aggregate MD simulation.

**Analysis.** Analyses of the generated trajectories were conducted using the *ptraj* module of AMBER, including generation of average water molecule number densities in the TcTS active site. This approach performs a root-mean-square fit of all atoms of the protein to the first frame, followed by construction of a grid around the protein, and, at 20 ps intervals, counts whether the center of the atom of interest is within a particular volume element (0.5 Å<sup>3</sup> each). The water number densities were viewed using Chimera<sup>50</sup> and contoured at a number density of 60 hits per element.

Binding free energies were estimated using the MM/PBSA method.<sup>51</sup> The single-trajectory approach was employed, such that the snapshot coordinates for both the bound and unbound states were obtained at 80 ps intervals from a single MD simulation. Poisson–Boltzmann solvation contributions were calculated using an  $\epsilon_{\text{in}}$  of 4 and an  $\epsilon_{\text{out}}$  of 80. The nonpolar contributions to the solvation energy were calculated using the  $\sigma$  decomposition scheme of Tan et al.<sup>52</sup> Solute entropy contributions were neglected in these calculations, as accurate computation of relative solute entropies is known to be problematic.<sup>53</sup> Consequently, we consider the binding affinities computed here to be only semiquantitative, but they can provide valuable insights into those factors governing association of Mu and lactose with enzyme.

## RESULTS

Using MD simulation, we have examined the behavior of the TcTS covalent intermediate with either Mu or lactose present in the acceptor site (right-hand side of Scheme 1a). In total, 18 MD simulations of TcTS were performed as 40 ns triplicates,

for apo presialylated TcTS, for the TcTS covalent intermediate with the acceptor site unoccupied, and for TcTs with the acceptor site occupied by Mu or lactose (Table S1 of the Supporting Information). When the acceptor site is unoccupied, initial outward and inward orientations of Tyr119 in that site were modeled (see Methods). The 18 MD simulations equilibrate with converged backbone root-mean-square deviations of ~1–3 Å (Figure S1 of the Supporting Information).

**Control Simulations of TcTS and Sialyl-TcTS.** Prior to analysis of the simulations of the covalent intermediate with Mu or lactose, we briefly consider reference simulations of presialylated and sialylated TcTS with an unoccupied acceptor site. Specifically, we consider the acceptor site flexibility and degree of solvent ordering.

An important aspect of TcTS acceptor site flexibility is the movement of Tyr119, which can adopt inward or outward orientations. Both inward and outward orientations of Tyr119 are found in apo TcTS crystal structures (see Methods) and are modeled as initial structures here, for both apo and sialylated TcTS simulations. For simulations of apo and sialylated TcTS initiated from an outward Tyr119 orientation, as required for binding acceptor β-galactoside glycoconjugates, we find sampling of both inward and outward orientations of Tyr119 (Figure 2a,c). We also observe the population of a third minor orientation, with a  $\chi_1$  value of 60° (Figure 2a,c) that corresponds to a rotated, stacking pose for Tyr119, which we label outward' (Figure 1b). Outward and outward' conformations appear to interact with lactose to a similar, favorable degree (Figure S2 of the Supporting Information).

It is clear, however, that in the later stages of the apo and sialylated TcTS trajectories, an inward orientation of Tyr119 is preferred, with only periodic excursions into an outward or outward' orientation (Figure S3a,c of the Supporting Information). The stability of this Tyr119 inward pose is underlined by the simulations of apo and sialylated TcTS initiated in the inward orientation, which remain entirely in that orientation over the course of the trajectories (Figure 2b,d and Figure S3b,d of the Supporting Information). In this inward conformation, Trp120 makes a T-shaped CH–π interaction with Tyr119 (Figure 1c), having an average centroid–CH distance of ~2.85 Å (Figure S4 of the Supporting Information), each such interaction resulting in a stabilizing dispersive interaction<sup>54</sup> of 2–3 kcal/mol. Rotation of Tyr119 to the outward position results in an increased distance between the aromatic rings of these residues, resulting in a loss of this stabilization. Simulations<sup>33</sup> of the catalytic N-terminal domain of the sialyl-TcTS system initiated in the inward conformation of Tyr119 also revealed that this inward conformation was maintained (initiation from the outward pose was not considered for the apo form).

An indicator of the openness of the acceptor site of TcTS, governed mainly by the Trp312 loop, is indicated by the Tyr119–Trp312 intercentroid distance. For apo TcTS simulations, the intercentroid distances vary between 6 and 20 Å (Figure 3a,b). For sialylated TcTS, the opening of the active site cleft is more muted, with a range of 5–15 Å for the intercentroid distance (Figure 3c,d). We note in broad terms that the Tyr119–Trp312 ring intercentroid distance is greater when the Tyr119 orientation is inward (compare, for example, Figure S3c of the Supporting Information and Figure 3c, before and after 10 ns, for the replicate in black). This reduced flexibility was also observed previously from simulations of the truncated sialyl-TcTS system<sup>33</sup> and was linked to a stabilizing

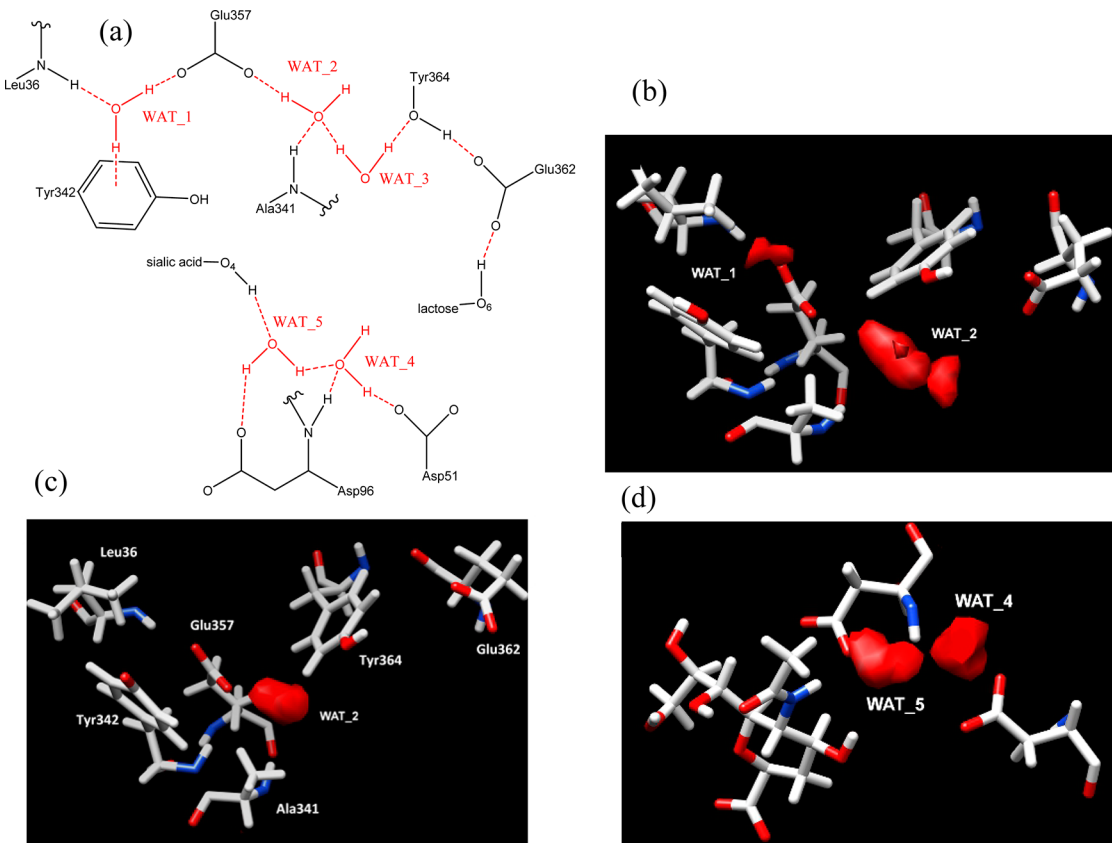


**Figure 4.** (a) Water sites WAT<sub>1</sub>–WAT<sub>5</sub> identified from molecular dynamics simulations. Contoured average water molecule densities (red) for (b) apo TcTS sites WAT<sub>1</sub> and WAT<sub>2</sub>, (c) sialylated TcTS site WAT<sub>2</sub>, and (d) sialylated TcTS sites WAT<sub>4</sub> and WAT<sub>5</sub>.

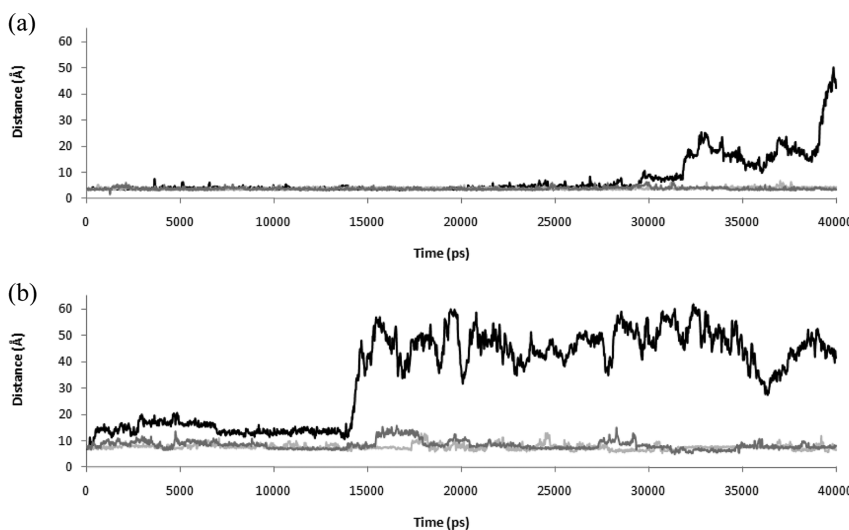


**Figure 5.** Distances (in Ångstroms) between the centers of mass of sialyl residues of sialylated TcTS and (a) lactose or (b) 4-methylumbelliflorone during three replicate MD simulations (black, light gray, and dark gray).

hydrogen bond with Arg314, which is similarly observed here (data not shown).

Finally, we consider the degree to which water is ordered in the TcTS active site from these explicit solvent MD simulations. In the apo TcTS trajectories, as indicated by contoured water number density, we observe some localization of water at two main sites: site WAT<sub>1</sub> is adjacent to residues Leu36, Tyr342, and Glu357 (Figure 4a,b; plots for replicate simulations are reported in Figure S5 of the Supporting

Information); there is also partial population of a second water site, WAT<sub>2</sub>, which sits between Glu357 and Ala341 (Figure 4a and Figure S5 of the Supporting Information). However, upon sialylation of TcTS, the WAT<sub>1</sub> site is physically obstructed by the sialyl residue and is absent (Figure 4c and Figure S5 of the Supporting Information). The carboxylate side chain of the Glu357 residue is now free to participate in hydrogen bonding interactions with the occupant of water site WAT<sub>2</sub>, which is seen to reside in this position for lifetimes

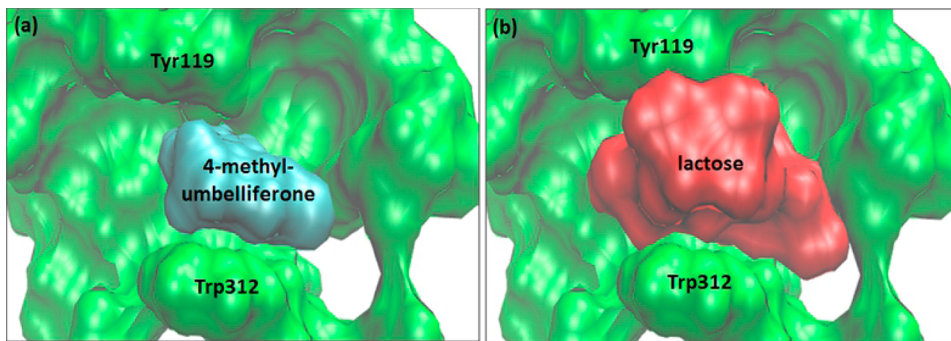


**Figure 6.** Space-filling representation of the acceptor site of sialylated TcTS (green) occupied by (a) 4-methylumbelliferone (cyan) and (b) lactose (red).

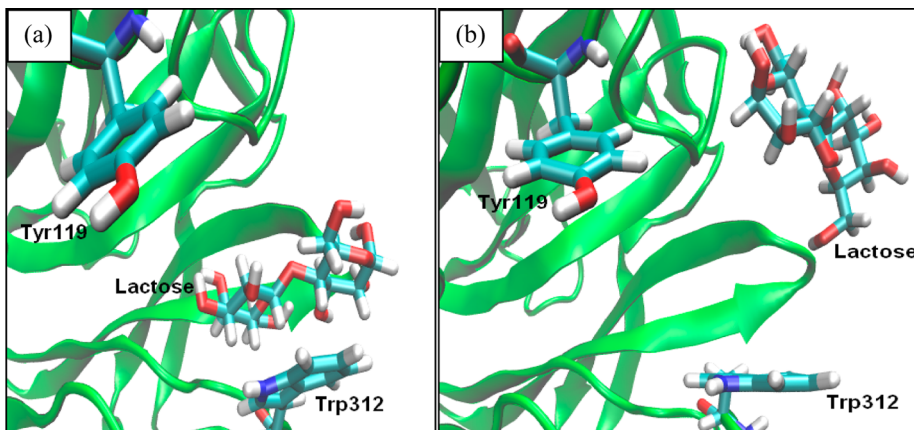


**Figure 7.** Selected steps from along the MD trajectory of the sialyl-TcTS–lactose complex. Initially, Tyr119 is outward and the Trp312 loop is closed (see Figure 1a). (a) At 22 ns, Tyr119 rotates away into an outward' pose, followed by a Trp312 motion to shift the Trp312–lactose portion of the stack. (b) Full opening of the Trp312 loop allows lactose to vacate the active site by 32 ns.

between 10 and 40 ns (Figure 4c). Therefore, only after sialylation of TcTS is a water molecule consistently found in position WAT<sub>2</sub>, over all six replicate simulations of this system (Figure 4c and Figure S6 of the Supporting Information). For sialylated TcTS, two other conserved regions of water occupancy, sites WAT<sub>4</sub> and WAT<sub>5</sub>, are found (Figure 4d and Figure S7 of the Supporting Information). WAT<sub>5</sub> interacts directly with the C4 hydroxyl of the sialyl residue. Evidently, a more extensive hydrogen bond network that involves water molecules is found in the sialylated system. This is a function of the polar nature of this residue and is potentially a contributor to the reduced flexibility in the sialylated form of the active site.

**Sialyl-TcTS with Lactose.** We now consider the three replicate MD simulations of sialyl-TcTS with lactose in the acceptor site. During the majority of the simulations, lactose remains close to the sialyl residue, with a short distance between the center of mass of the TcTS-bound sialyl moiety and the lactose of ~4 Å (Figure 5a). This proximity corresponds, from inspection, to a well-defined bound pose in the acceptor site, where lactose stacks against Tyr119 and Trp312 (Figure 6). By virtue of this stacking interaction, Tyr119 remains mainly in an outward conformation, with a  $\chi_1$  value of  $-60^\circ$  (Figure S3e of the Supporting Information). The cohesion of the Trp312–lactose–Tyr119 motif is also illustrated by a low degree of fluctuation in the Trp312–Tyr119 intercentroid distance, which remains at ~9 Å (Figure 3e). This short distance suggests that a significant opening of

the Tyr119/Trp312 acceptor site, which could have allowed greater solvent exposure of the active site, does not occur.

Using the MM/PBSA method, we obtain an indication of the strength and nature of the interaction energetics between lactose and TcTS (Table S2 of the Supporting Information). In this analysis, only configurations with an occupied acceptor site were used. The computed total binding free energy for lactose, averaged over the three replicate simulations, is  $-60.1$  kcal/mol. The steric complementarity between lactose and Trp312 or Tyr119 is highlighted by the significant van der Waals component of this interaction, with a  $\Delta E_{\text{vdw}}$  contribution to binding of  $-27.5$  kcal/mol (Table S2 of the Supporting Information). The remaining binding affinity is principally caused by a significant nonpolar solvation term of  $-33.3$  kcal/mol; this sizable term reflects the relative benefit of desolvation of Tyr119 and Trp312 compared to the (mainly) polar lactose, according to the model of Tan et al.<sup>52</sup> Indeed, the electrostatic contributions to binding are rather small [ $<10$  kcal/mol in magnitude (Table S2 of the Supporting Information)] and reflect the mainly nonpolar nature of the association.

For one of the three trajectories, lactose is seen to depart from the protein active site. This event occurs at  $\sim 31.5$  ns, as indicated by the distance between the center of mass of the lactose and the sialyl residue of the TcTS covalent intermediate (Figure 5a). This was observed in a replicate of our previous simulation of the sialyl-TcTS–lactose complex.<sup>32</sup> Interestingly, in these new simulations, at the same time as this lactose dissociation event, we observe rotation of Tyr119 from outward

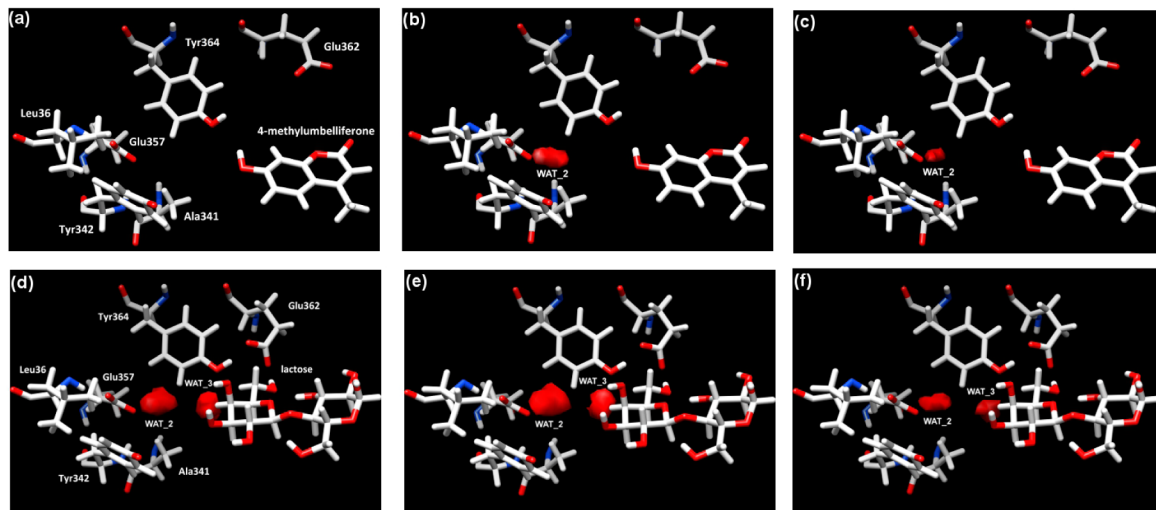


**Figure 8.** Contoured average water molecule number densities (red) for three replicate simulations of sialylated TcTS systems complexed with 4-methylumbelliflone (a–c) and lactose (d–f).

to outward' (Figure S3e of the Supporting Information and Figure 7). Although an outward to outward' transition is observed, only a slight opening of the acceptor site occurs, to  $\sim 10\text{--}12 \text{ \AA}$  (Figure 3e).

As with the sialylated protein in the absence of lactose, multiple distinct sites of water occupancy are observed here. Indeed, the same WAT\_2 site (Figure 8) and WAT\_4 and WAT\_5 sites are occupied. Notably, however, additional water is found to localize at a new site, WAT\_3, in all three replicate simulations (Figure 8). Water at this site is within hydrogen bonding distance of Tyr364, which hydrogen bonds to Glu362, which in turn interacts with lactose (Figure 4a).

**Sialyl-TcTS with Mu.** Interestingly, the simulated behavior of Mu in the acceptor site of sialylated TcTS is quite different from that of lactose. In one of the replicate simulations, departure of Mu is observed; this occurs considerably earlier in the simulation [at  $\sim 13 \text{ ns}$  (Figure 5b)] than with lactose [at  $\sim 31.5 \text{ ns}$  (Figure 5a)]. Weaker interactions between Mu and the acceptor site are suggested by inspection of these trajectories that indicate that Mu adopts a multiplicity of transient poses in the active site of TcTS, for example, making bimolecular contacts with residues Tyr119, Trp312, and Ser122 (Figure S8 of the Supporting Information). Indeed, the dimensions of Mu do not seem to be capable of spanning the distance required to satisfactorily stack with Tyr119 and Trp312 simultaneously (Figure 6). Even when Mu does depart, it remains nonspecifically associated with the protein surface, via residues Arg311 (Figure S8d of the Supporting Information) and Phe58 (Figure S9 of the Supporting Information).

With regard to acceptor site openness, the Trp312–Tyr119 intercentroid distance ranges from 6 to 15  $\text{\AA}$  (Figure 3f). This range is similar to that found for MD of sialylated TcTS without a leaving group present (Figure 3c,d) and points to considerable opening, and solvent exposure, of the acceptor site. We also observe sampling of inward, outward, and outward' Tyr119 poses during the trajectories (Figure 2f and Figure S3f of the Supporting Information). We note that the inward conformations are sampled only after the departure of Mu from the acceptor site.

The lower affinity of Mu–acceptor site interactions is reflected by MM/PBSA interaction energetics (Table S2 of

the Supporting Information). For bound configurations of Mu, the computed total binding free energy for lactose is  $-31.4 \text{ kcal/mol}$ , approximately half that of lactose. This is a result of a combination of a weaker van der Waals interaction with the protein ( $-15.1 \text{ kcal/mol}$ ) and a less favorable nonpolar desolvation energy. The latter is most likely a result of a less occluded nonpolar acceptor site, arising from the reduced steric complementarity and size of Mu. Here, association of the nonpolar substrate with the nonpolar active site is reflected by even smaller electrostatic contributions to the binding than is predicted for lactose [ $<4 \text{ kcal/mol}$  in magnitude (Table S2 of the Supporting Information)].

Finally, we consider the extent of water localization in the active site of the sialyl-TcTS–Mu complex. Concomitant with the ill-defined poses of Mu, water similarly is disordered. Thus, there is little population of the WAT\_2 site adjacent to Glu357 and Ala341 and no population of the WAT\_3 site next to WAT\_2 and Tyr364 (Figure 8a–c). The greater mobility of Mu in the active site and larger opening of the active site appear to disrupt water localization and promote its mobility. The smaller spatial extent of Mu also leaves a greater volume in the active site for water to occupy. The well-defined occupation of the acceptor site by lactose near Tyr342 and in particular sialyl C2 contrasts with the larger ligand-free volume in the Mu-occupied TcTS acceptor site (Figure 8).

## ■ DISCUSSION AND CONCLUSIONS

In this work, we have sought to probe the effect of protein conformational flexibility on the observed stronger preference for hydrolysis when the substrate is MuNANA rather than sialyllactose (Table 1). From our MD simulations, we observe markedly different behavior for sialylated TcTS depending on whether the lactose or Mu moiety occupies the acceptor site.

When lactose occupies the acceptor site, a well-defined noncovalently bound complex is observed. Computed binding energetics suggest good steric lactose–acceptor site packing and a significant hydrophobic driving force as lactose forges CH– $\pi$  and OH– $\pi$  interactions with nonpolar Trp312 and Tyr119 residues. The MD simulations predict that the acceptor site remains in a closed and less solvent accessible conformation relative to unliganded apo and sialylated TcTS. The distinct water sites localized in the covalent intermediate active site in

the absence of lactose are also observed with lactose present; when lactose binds, an additional site also forms [WAT\_3 (Figure 4c)], which indirectly is involved in interactions with lactose (Figure 4a). We note that sites WAT\_2 and WAT\_3 do not reside near Asp59 or sialyl C2 and therefore would not be potential candidates as the water of hydrolysis for attack at that carbon. Instead, these water sites are part of a hydrogen bonding network that contributes to the stable, well-defined pose adopted by lactose in the TcTS acceptor site. Lactose is thus predicted to persist in a ternary stacking orientation with two aromatic active site residues, maintaining a hydrophobic environment and apparently protecting the covalent intermediate from hydrolysis at a point when solvent exposure of the catalytic cleft would be expected to be at its most sensitive.

When Mu rather than lactose is present in the acceptor site, the MD simulations suggest a rather different behavior. First, Mu does not adopt a single, stable pose in the acceptor site but explores a range of binding orientations. This appears at least in part to be a consequence of its inability, in contrast to lactose, to fully span the Tyr119–Trp312 recognition motif (Figure 6). Indeed, energetic analysis via MM/PBSA suggests that Mu is bound to approximately half of the extent of lactose and makes weaker van der Waals contacts with the protein. For both lactose and Mu, the product leaves the acceptor site for one of the three replicate MD simulations, although this occurs considerably earlier in the trajectory for Mu (Figure 5).

One suggested hypothesis for the more favorable hydrolysis of MuNANA is that the occlusion of the acceptor site by the Mu moiety inhibits the correct orientation of an inbound acceptor molecule and/or Tyr119, required for the successful transfer of the sialyl group to an acceptor molecule.<sup>17</sup> From our simulations, however, it does not appear that Mu unduly inhibits the flexibility of Tyr119. Although disordered in pose, Mu still may interfere with acceptor binding; however, Mu is found to fully depart from the protein active site quite readily, as observed in one of the replicate trajectories.

A second observation from our sialyl-TcTS–Mu simulations is that there is greater degree of opening of the acceptor site compared to that of the sialyl-TcTS–lactose system. An opening with a Tyr119–Trp312 intercentroid distance up to 15 Å is found in the former, similar to that of simulated TcTS without the acceptor site ligand (up to 20 Å). A wider opening of the acceptor site, which sits at the mouth of the active site, leads to a greater level of solvent exposure. Interestingly, the active site water seems more disordered in the presence of Mu, with only partial occupation of the WAT\_2 site and the absence of the WAT\_3 site, which formed part of the network that binds lactose. The weaker interaction with Mu and the resulting greater flexibility of the covalent intermediate appear to arise from the lower acceptor site complementarity to the dimensions of the flatter, shorter Mu molecule (Figure 6). Greater access is available for water, which is less structured (Figure 8a–c), to attack at C2 on the TcTS-bound sialyl residue (Scheme 1c); this would seem to be conducive to hydrolysis relative to the more ordered, less open active site when lactose is bound. In a vein similar to that of our simulations of sialyl-TcTS with Mu and lactose, recent MD simulations pointed to greater active site opening for the hydrolyzing enzyme *Trypanosoma rangeli* sialidase (TrSA) relative to that of TcTS.<sup>33</sup> This was a proposed contributor to its hydrolyzing activity. In TrSA, the substitution of Tyr119 with Ser is key to preferential hydrolysis.

Experimental studies with TcTS find that transfer efficiency depends on the identity of the sialyl donor aglycon.<sup>26</sup> These studies suggest that, in general, transferase activity is poorer when the donor aglycon is not a carbohydrate: in a surface plasmon resonance study of the transfer rates of various sialyl donors and sialyl acceptors with *Trypanosoma brucei* and *Trypanosoma congoense trans-sialidases*, greater transfer ability was found with a sialyllactose donor rather than MuNANA.<sup>55,56</sup> In these systems, as predicted here for TcTS, there may again be weaker ordering and greater solvent accessibility of the protein by a noncarbohydrate aglycon, leading to less efficient transfer. While we propose that protein flexibility can contribute to the relative preference of a substrate for hydrolysis versus transfer, future work is required to explore the full potential energy surface using quantum chemical techniques to model the energetics of these competing reactions.

In conclusion, on the basis of this study, we concur with Paris et al.,<sup>31</sup> who, in their crystallographic and protein engineering study to convert *T. rangeli* sialidase into a *trans*-sialidase, commented that “the presence of a sugar acceptor binding site, the fine tuning of protein-substrate interactions and the flexibility of crucial active site residues are all important to achieve *trans*-glycosidase activity”. A deeper understanding of the molecular recognition and dynamics of TcTS afforded by this study provides information that could be useful in the challenging pursuit of therapeutics effective against Chagas disease, for example, targeting specific protein conformational substates and/or leveraging preferential water binding locations.

## ASSOCIATED CONTENT

### S Supporting Information

Tables S1 and S2 and Figures S1–S9 include simulation details, computed binding energies, MD time series of backbone root-mean-square deviations, key interaction distances and amino acid dihedrals involving TcTS, and TcTS active site water maps. This material is available free of charge via the Internet at <http://pubs.acs.org>.

## AUTHOR INFORMATION

### Corresponding Author

\*E-mail: R.A.Bryce@manchester.ac.uk. Fax: +44 (0)161 275 2481. Telephone: +44 (0) 161 275 8345.

### Present Address

<sup>§</sup>Global Health Institute, École Polytechnique Fédérale de Lausanne, CH-1015 Lausanne, Switzerland.

### Funding

We thank EPSRC and Johnson & Johnson, Pharmaceutical Research and Development, a division of Janssen Pharmaceutica N.V., for funding.

### Notes

The authors declare no competing financial interest.

## ACKNOWLEDGMENTS

We acknowledge the use of the UK National Grid Service and the National Service for Computational Chemistry Software in conducting this work.

## ABBREVIATIONS

TcTS, *T. cruzi trans-sialidase*; TrSA, *T. rangeli sialidase*; MD, molecular dynamics; MuNANA, 4-methylumbelliferyl  $\alpha$ -D-acetyleneuraminate.

## REFERENCES

- (1) Fischer, E. (1894) Einfluss der configuration auf die wirkung der enzyme. *Ber. Dtsch. Chem. Ges.* 27, 2985–2993.
- (2) Koshland, D. E., and Neet, K. E. (1968) Catalytic and regulatory properties of enzymes. *Annu. Rev. Biochem.* 37, 359–410.
- (3) Ma, B., and Nussinov, R. (2010) Enzyme dynamics point to stepwise conformational selection in catalysis. *Curr. Opin. Chem. Biol.* 14, 652–659.
- (4) Paris, G., Cremona, M. L., Amaya, M. F., Buschiazza, A., Giambiagi, S., Frasch, A. C., and Alzari, P. M. (2001) Probing molecular function of trypanosomal sialidases: Single point mutations can change substrate specificity and increase hydrolytic activity. *Glycobiology* 11, 305–311.
- (5) Schenkman, S., Jiang, M. S., Hart, G. W., and Nussenzweig, V. (1991) A novel cell surface *trans-sialidase* of *Trypanosoma cruzi* generates a stage-specific epitope required for invasion of mammalian cells. *Cell* 65, 1117–1125.
- (6) Hall, B. F., Webster, P., Ma, A. K., Joiner, K. A., and Andrews, N. W. (1992) Desialylation of lysosomal membrane-glycoproteins by *Trypanosoma cruzi*: A role for the surface neuraminidase in facilitating parasite entry into the host-cell cytoplasm. *J. Exp. Med.* 176, 313–325.
- (7) Burleigh, B. A., and Andrews, N. W. (1995) The mechanisms of *Trypanosoma cruzi* invasion of mammalian cells. *Annu. Rev. Microbiol.* 49, 175–200.
- (8) Clayton, J. (2010) Chagas disease 101. *Nature* 465, S4–S5.
- (9) Previato, J. O., Andrade, A. F., Pessolani, M. C., and Mendonça-Previato, L. (1985) Incorporation of sialic acid into *Trypanosoma cruzi* macromolecules. A proposal for a new metabolic route. *Mol. Biochem. Parasitol.* 16, 85–96.
- (10) Schenkman, S., Ferguson, M. A., Heise, N., de Almeida, M. L., Mortara, R. A., and Yoshida, N. (1993) Mucin-like glycoproteins linked to the membrane by glycosylphosphatidylinositol anchor are the major acceptor of sialic acid in a reaction catalyzed by *trans-sialidase* in metacyclic forms of *Trypanosoma cruzi*. *Mol. Biochem. Parasitol.* 59, 293–303.
- (11) Pereira-Chioccola, V. L., Acosta-Serrano, A., Correia de Almeida, I., Ferguson, M. A., Souto-Padron, T., Rodrigues, M. M., Travassos, L. R., and Schenkman, S. (2000) Mucin-like molecules form a negatively charged coat that protects *Trypanosoma cruzi* trypomastigotes from killing by human anti- $\alpha$ -galactosyl antibodies. *J. Cell Sci.* 113, 1299–1307.
- (12) Engstler, M., Reuter, G., and Schauer, R. (1993) Enzymatic characterisation and possible biological significant of *trans-sialidase* from *Trypanosoma brucei*. *Glycoconjugate J.* 10, 287.
- (13) Parodi, A. J., Pollevick, G. D., Mautner, M., Buschiazza, A., Sanchez, D. O., and Frasch, A. C. (1992) Identification of the gene(s) coding for the *trans-sialidase* of *Trypanosoma cruzi*. *EMBO J.* 11, 1705–1710.
- (14) Schenkman, S., De Carvalho, L. P., and Nussenzweig, V. (1992) *Trypanosoma cruzi trans-sialidase* and neuraminidase activities can be mediated by the same enzymes. *J. Exp. Med.* 175, 567–575.
- (15) Medina-Acosta, E., Franco, A. M., Jansen, A. M., Sampol, M., Neves, N., Pontes-de-Carvalho, L., Grimaldi Junior, G., and Nussenzweig, V. (1994) *Trans-sialidase* and sialidase activities discriminate between morphologically indistinguishable trypanosomes. *Eur. J. Biochem.* 225, 333–339.
- (16) Haselhorst, T., Wilson, J. C., Liakatos, A., Kiefel, M. J., Dyason, J. C., and von Itzstein, M. (2004) NMR spectroscopic and molecular modeling investigations of the *trans-sialidase* from *Trypanosoma cruzi*. *Glycobiology* 14, 895–907.
- (17) Benkovic, S. J., and Hammes-Schiffer, S. (2003) A perspective on enzyme catalysis. *Science* 301, 1196–1202.
- (18) Newstead, S. L., Watson, J. N., Bennet, A. J., and Taylor, G. (2005) Galactose recognition by the carbohydrate-binding module of a bacterial sialidase. *Acta Crystallogr. D61*, 1483–1491.
- (19) Amaro, R. E., Minh, D. D., Cheng, L. S., Lindstrom, W. M., Olson, A. J., Lin, J. H., Li, W. W., and McCammon, J. A. (2007) Remarkable loop flexibility in avian influenza N1 and its implications for antiviral drug design. *J. Am. Chem. Soc.* 129, 7764–7765.
- (20) Chavas, L. M., Tringali, C., Fusi, P., Venerando, B., Tettamanti, G., Kato, R., Monti, E., and Wakatsuki, S. (2005) Crystal structure of the human cytosolic sialidase neu2: Evidence for the dynamic nature of substrate recognition. *J. Biol. Chem.* 280, 469–475.
- (21) Amaya, M. F., Watts, A. G., Damager, I., Wehenkel, A., Nguyen, T., Buschiazza, A., Paris, G., Frasch, A. C., Wither, S. G., and Alzari, P. M. (2004) Structural insights into the catalytic mechanism of *Trypanosoma cruzi trans-sialidase*. *Structure* 12, 775–784.
- (22) Masukawa, K. M., Kollman, P. A., and Kuntz, I. D. (2003) Investigation of neuraminidase-substrate recognition using molecular dynamics and free energy calculations. *J. Med. Chem.* 46, 5628–5637.
- (23) Damager, I., Buchini, S., Amaya, M. F., Buschiazza, A., Alzari, P., Frasch, A. C., Watts, A., and Withers, S. G. (2008) Kinetic and mechanistic analysis of *Trypanosoma cruzi trans-sialidase* reveals a classical ping-pong mechanism with acid/base catalysis. *Biochemistry* 47, 3507–3512.
- (24) Watts, A. G., Damager, I., Amaya, M. L., Buschiazza, A., Alzari, P., Frasch, A. C., and Withers, S. G. (2003) *Trypanosoma cruzi trans-sialidase* operates through a covalent sialyl-enzyme intermediate: Tyrosine is the catalytic nucleophile. *J. Am. Chem. Soc.* 125, 7532–7533.
- (25) Ferrero-Garcia, M. A., Trombetta, S. E., Sánchez, D. O., Reglero, A., Frasch, A. C., and Parodi, A. J. (1993) The action of *Trypanosoma cruzi trans-sialidase* on glycolipids and glycoproteins. *Eur. J. Biochem.* 213, 765–771.
- (26) Vandekerckhove, F., Schenkman, S., Pontes de Carvalho, L., Tomlinson, S., Kiso, M., Yoshida, M., Hasegawa, A., and Nussenzweig, V. (1992) Substrate-specificity of the *Trypanosoma cruzi trans-sialidase*. *Glycobiology* 2, 541–548.
- (27) Todeschini, A. R., Mendonça-Previato, L., Previato, J. O., Varki, A., and van Halbeek, H. (2000) Trans-sialidase from *Trypanosoma cruzi* catalyzes sialoside hydrolysis with retention of configuration. *Glycobiology* 10, 213–221.
- (28) Neres, J., Brewer, M., Ratier, L., Edwards, P. N., Botti, H., Buschiazza, A., Alzari, P. M., Frasch, A. C. C., Bryce, R. A., and Douglas, K. T. (2009) Discovery of novel inhibitors of *Trypanosoma cruzi trans-sialidase* from in silico screening. *Bioorg. Med. Chem. Lett.* 19, 589–596.
- (29) Neres, J., Bryce, R. A., and Douglas, K. T. (2008) Rational drug design in parasitology: *trans-Sialidase* as a case study for Chagas disease. *Drug Discovery Today* 13, 110–117.
- (30) Neres, J. P., Bonnet, P., Edwards, P. N., Kotian, P. L., Buschiazza, A., Alzari, P. M., Bryce, R. A., and Douglas, K. T. (2007) Benzoic acid and pyridine derivatives as inhibitors of *Trypanosoma cruzi trans-sialidase*. *Bioorg. Med. Chem.* 15, 2106–2119.
- (31) Paris, G., Ratier, L., Amaya, M. F., Nguyen, T., Alzari, P. M., and Frasch, A. C. (2005) A sialidase mutant displaying *trans-sialidase* activity. *J. Mol. Biol.* 345, 923–934.
- (32) Mitchell, F. L., Miles, S. M., Neres, J., Bichenkova, E. V., and Bryce, R. A. (2010) Tryptophan as a molecular shovel in the glycosyl transfer activity of *Trypanosoma cruzi trans-sialidase*. *Biophys. J.* 98, L38–L40.
- (33) Demir, O., and Roitberg, A. (2009) Modulation of catalytic function by differential plasticity of the active site: Case study of *Trypanosoma cruzi trans-sialidase* and *Trypanosoma rangeli sialidase*. *Biochemistry* 48, 3398–3406.
- (34) Hillier, I. H. (1999) Chemical reactivity studied by hybrid QM/MM methods. *THEOCHEM* 463, 45–52.
- (35) Fong, P., McNamara, J. P., Hillier, I., and Bryce, R. A. (2009) Assessment of QM/MM scoring functions for molecular docking to HIV-1 protease. *J. Chem. Inf. Model.* 49, 913–924.

- (36) Case, D. A., Darden, T. A., Cheatham, T. E., III, Simmerling, C. L., Wang, J., Duke, R. E., Luo, R., Merz, K. M., Pearlman, D. A., Crowley, M., Walker, R. C., Zhang, W., Wang, B., Hayik, S., Roitberg, A., Seabra, G., Wong, K. F., Paesani, F., Wu, X., Brozell, S., Tsui, V., Gohlke, H., Yang, L., Tan, C., Mongan, J., Hornak, V., Cui, G., Beroza, P., Mathews, D. H., Schafmeister, C., Ross, W. S., and Kollman, P. A. (2006) AMBER 9, University of California, San Francisco.
- (37) Molecular Operating Environment (MOE), version 2009.10 (2009) Chemical Computing Group, Inc.: Quebec City, QC.
- (38) Sybyl Molecular Modelling Package, version 6.6 (1999) Tripos Inc., St. Louis.
- (39) Buschiazzo, A., Amaya, M. F., Cremona, M. L., Frasch, A. C., and Alzari, P. M. (2002) The crystal structure and mode of action of *trans*-sialidase, a key enzyme in *Trypanosoma cruzi* pathogenesis. *Mol. Cell* 10, 757–768.
- (40) Vriend, G. (1990) What If: A Molecular Modeling and Drug Design Program. *J. Mol. Graphics* 8, 52–56.
- (41) Jorgensen, W. L., Chandrasekhar, J., Madura, J. D., Impey, R. W., and Klein, M. L. (1983) Comparison of simple potential functions for simulating liquid water. *J. Chem. Phys.* 79, 926–935.
- (42) Duan, Y., Wu, C., Chowdhury, S., Lee, M. C., Xiong, G., Zhang, W., Yang, R., Cieplak, P., Luo, R., Lee, T., Caldwell, J., Wang, J., and Kollman, P. (2003) A point-charge force field for molecular mechanics simulations of proteins based on condensed-phase quantum mechanical calculations. *J. Comput. Chem.* 24, 1999–2012.
- (43) Kirschner, K. N., Yongye, A. B., Tschampel, S. M., González-Outeirño, J., Daniels, C. R., Foley, B. L., and Woods, R. J. (2008) GLYCAM06: A generalizable biomolecular force field. *Carbohydrates. J. Comput. Chem.* 29, 622–655.
- (44) Wang, J., Cieplak, P., and Kollman, P. A. (2000) How well does a restrained electrostatic potential (RESP) model perform in calculating conformational energies of organic and biological molecules? *J. Comput. Chem.* 21, 1049–1074.
- (45) Wang, J., Wolf, R. M., Caldwell, J. W., Kollman, P. A., and Case, D. A. (2004) Development and testing of a general Amber force field. *J. Comput. Chem.* 25, 1157–1174.
- (46) Essmann, U., Perera, L., and Berkowitz, M. L. (1995) A smooth particle mesh Ewald method. *J. Chem. Phys.* 103, 8577–8593.
- (47) Adelman, S. A., and Doll, J. D. (1976) Generalized Langevin equation approach for atom-solid-surface scattering: General formulation for classical scattering of harmonic solids. *J. Chem. Phys.* 64, 2375–2388.
- (48) Berendsen, H. J. C., Postma, J. P. M., van Gunsteren, W. F., DiNola, A., and Haak, J. R. (1984) Molecular dynamics with coupling to an external bath. *J. Chem. Phys.* 81, 3684–3690.
- (49) Ryckaert, J. P., Ciccotti, G., and Berendsen, H. J. C. (1977) Numerical-integration of Cartesian equations of motion of a system with constraints: Molecular-dynamics of N-alkanes. *J. Comput. Phys.* 23, 327–341.
- (50) Pettersen, E. F., Goddard, T. D., Huang, C. C., Couch, G. S., Greenblatt, D. M., Meng, E. C., and Ferrin, T. E. (2004) UCSF chimera: A visualization system for exploratory research and analysis. *J. Comput. Chem.* 25, 1605–1612.
- (51) Srinivasan, J., Cheatham, T. E., III, Cieplak, P., Kollman, P. A., and Case, D. A. (1998) Continuum solvent studies of the stability of DNA, RNA, and phosphoramidate-DNA helices. *J. Am. Chem. Soc.* 120, 9401–9409.
- (52) Tan, C., Tan, Y. H., and Luo, R. (2007) Implicit nonpolar solvent models. *J. Phys. Chem. B* 111, 12263–12274.
- (53) Brandsdal, B. O., Österberg, F., Almlöf, M., Feierberg, I., Luzhkov, V. B., and Åqvist, J. (2003) Free Energy Calculations and Ligand Binding. *Adv. Protein Chem.* 66, 123–158.
- (54) Raju, R. K., Ramraj, A., Vincent, M. A., Hillier, I. H., and Burton, N. A. (2008) Carbohydrate-protein recognition probed by density functional theory and ab initio calculations including dispersive interactions. *Phys. Chem. Chem. Phys.* 10, 6500–6508.
- (55) Engstler, M., Reuter, G., and Schauer, R. (1993) The developmentally regulated *trans*-sialidase from *Trypanosoma brucei* sialylates the procyclic acidic repetitive protein. *Mol. Biochem. Parasitol.* 61, 11–13.
- (56) Engstler, M., Schauer, R., and Brun, R. (1995) Distribution of developmentally regulated *trans*-sialidases in the Kinetoplastida and characterization of a shed *trans*-sialidase activity from procyclic *Trypanosoma congolense*. *Acta Trop.* 59, 117–129.